A Breathing Metal-Organic Framework Based on Flexible Inorganic Building Units

Supplementary Information

Erik Svensson Grape,[†] Hongyi Xu,[†] Ocean Cheung,[‡] Marion Calmels,[§] Jingjing Zhao,[†] Catherine Dejoie,[⊥] Davide M. Proserpio,[∥,▽] Xiaodong Zou,[†] A. Ken Inge*[,†]

[†]Department of Materials and Environmental Chemistry, Stockholm University, SE 106 91 Stockholm, Sweden

[‡]Division of Nanotechnology and Functional Materials, Department of Engineering Sciences, The Ångström Laboratory, Uppsala University, Box 534, SE-751 21 Uppsala, Sweden

[§]INSA Lyon – Département Sciences et Génie Des Matériaux, 69621 Villeurbanne Cedex, France

[∥] ESRF – the European Synchrotron Radiation Facility, CS40220, Grenoble 38043, France

[⊥]Dipartimento di Chimica, Università degli Studi di Milano, Milano, 20133, Italy

[▽]Samara Center for Theoretical Materials Science (SCTMS), Samara State Technical University, Samara 443100, Russia

Table of Contents

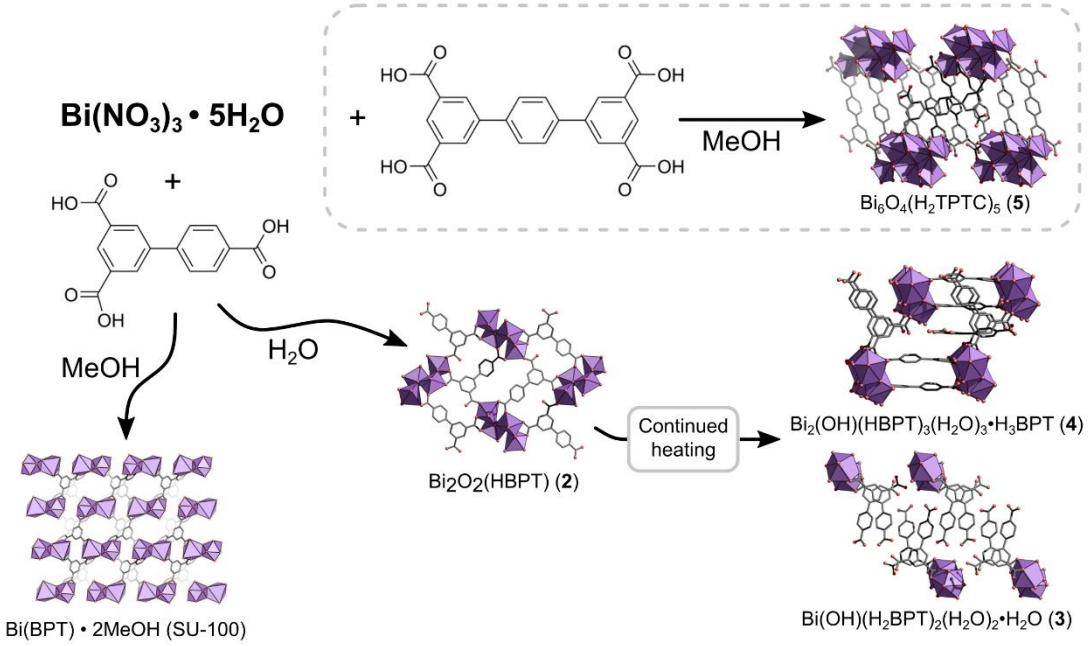

Figure S1. An overview of the syntheses performed in order to obtain the five coordination polymers. Four different phases are obtained with the H_3BPT linker, using either methanol (**1**) or water as a solvent (**2**-**4**). When using H_4TPTC, a single phase is obtained in methanol (**5**),

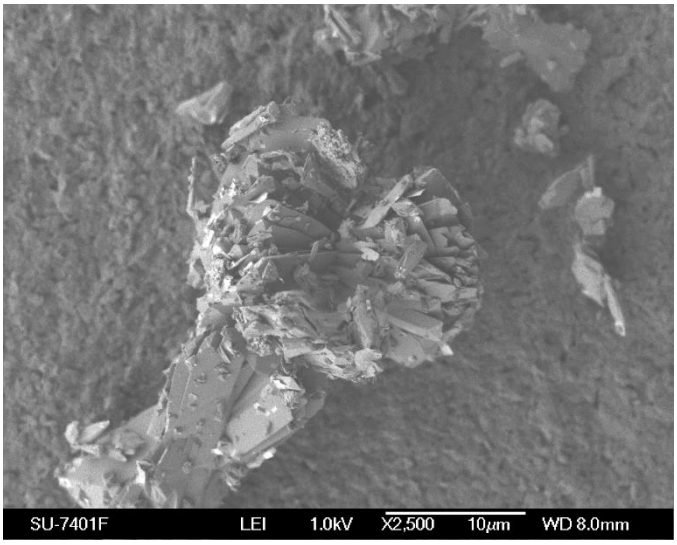

Figure S2. SEM micrograph of Bi(BPT)•$(MeOH)_2$ (SU-100), showing an aggregate of plate-like crystals.

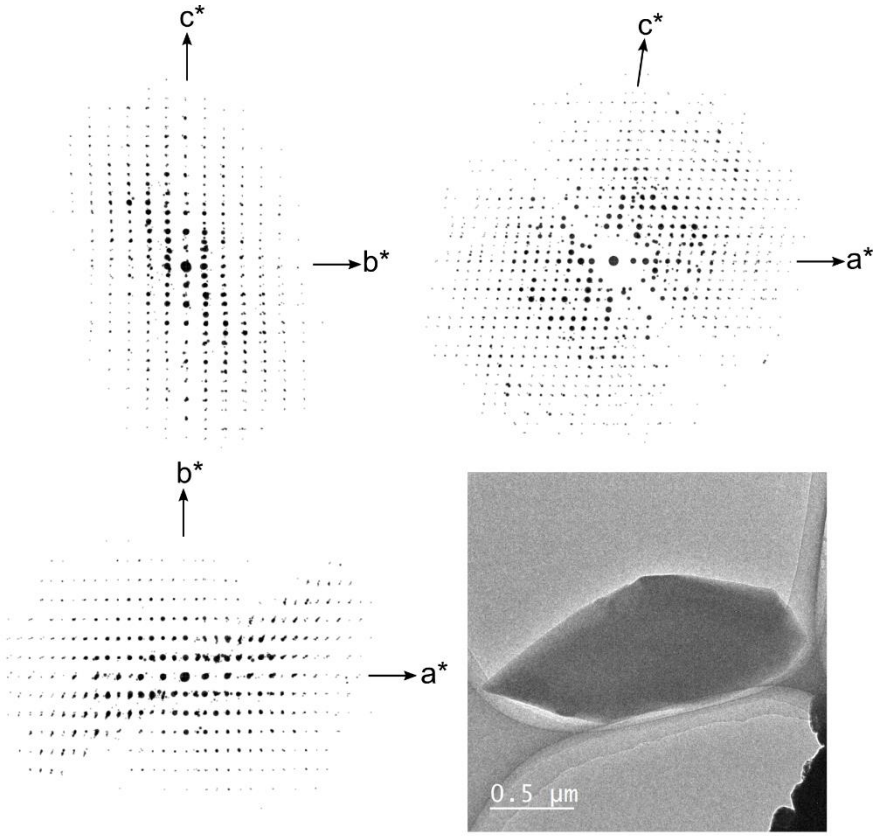

Figure S3. Reciprocal space projections along a*, b* and c*, as well as the crystal used for collecting the electron diffraction data on as-synthesized SU-100.

Table S1: Crystallographic table for electron diffraction data of as-synthesized SU-100.

Identification code	as-synthesized SU-100
Crystal system	Monoclinic
Space group	*I*2/*a* (No. 15)
Unit cell dimensions	*a* = 18.26 Å
	b = 10.32 Å
	c = 21.55 Å
	β = 97.2°
Volume (Å^3)	4029 Å^3
Z	8
Rotation range	82.34° (-70.15 to 12.19°)
Index ranges	-17 ≤ *h* ≤ 20
	-9 ≤ *k* ≤ 9
	-21 ≤ *l* ≤ 23
Reflections collected	4172
Independent reflections	1788
	[R(int) = 0.1702]
Completeness (to 1.0 Å resolution)	80.2 %
R_1 (ED model) [I > 2σ(I)]	0.2151

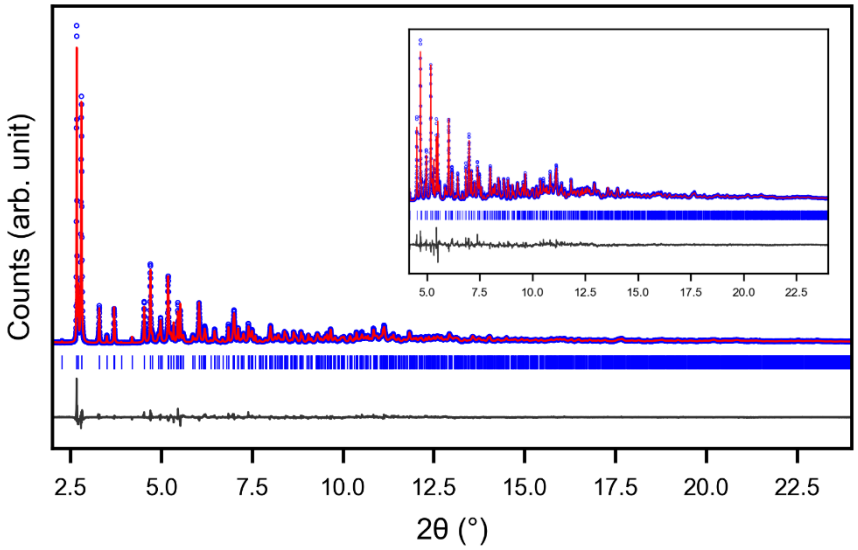

Figure S4. Plot for the refinement of Bi(BPT)•$(MeOH)_2$ (SU-100, as synthesized). High resolution XRPD data were collected at 11BM at the APS, Argonne National Laboratory, USA, λ = 0.412735 Å.

Table S2. Crystallographic details from X-ray powder diffraction data and structure refinement details for Bi(BPT)•$(MeOH)_2$ (SU-100, as synthesized).

Identification code	SU-100, as synthesized
Crystal system	Monoclinic
Space group	*I*2/*a* (No. 15)
Unit cell dimensions	*a* = 17.854(3) Å
	b = 9.613(2) Å
	c = 21.047(4) Å
	β = 96.771(2)°
Volume ($Å^3$)	3587(1) $Å^3$
Wavelength	0.412735 Å
Refinement method	Profile method
Refinement statistics	R_{wp} = 7.13 %
	GOF = 1.75

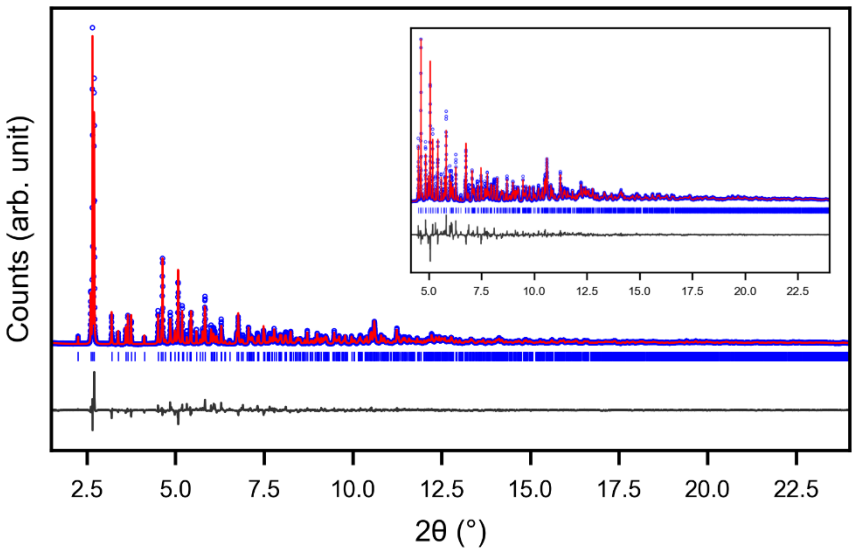

Figure S5. Plot for the refinement of Bi(BPT)•$(MeOH)_3$ (MeOH@SU-100). High resolution XRPD data were collected at 11BM at the APS, Argonne National Laboratory, USA, λ = 0.412735 Å.

Table S3. Crystallographic details from X-ray powder diffraction data and structure refinement details for Bi(BPT)•$(MeOH)_3$ (MeOH@SU-100).

Identification code	SU-100, MeOH
Crystal system	Monoclinic
Space group	*I*2/*a* (No. 15)
Unit cell dimensions	*a* = 18.0213(6) Å
	b = 10.0372(4) Å
	c = 21.2624(8) Å
	β = 99.206(1)°
Volume ($Å^3$)	3796.5(2) $Å^3$
Wavelength	0.412735 Å
Refinement method	Profile method
Refinement statistics	R_{wp} = 10.46 %
	GOF = 2.74

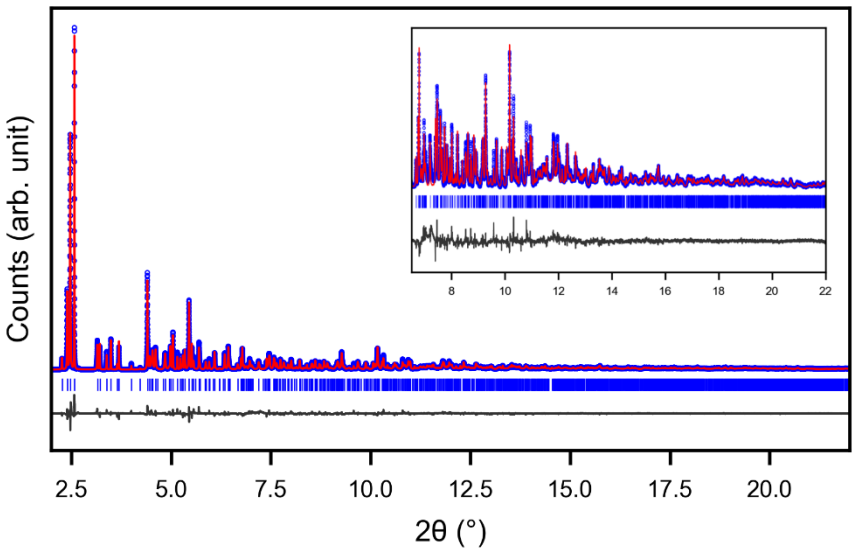

Figure S6. Plot for the refinement of Bi(BPT)•(DEF) (DEF@SU-100). High-resolution XRPD data were collected at ID22 at ESRF. Grenoble, France, λ = 0.40022674 Å.

Table S4. Crystallographic details from X-ray powder diffraction data and structure refinement details for Bi(BPT)•(DEF) (DEF@SU-100).

Identification code	SU-100-DEF
Crystal system	Monoclinic
Space group	*I*2/*a* (No. 15)
Unit cell dimensions	a = 18.018(1) Å
	b = 10.8566(8) Å
	c = 20.478(1) Å
	β = 99.1116(5)°
Volume (Å^3)	3955.5 Å^3
Wavelength	0.40022674 Å
Refinement method	Profile method
Refinement statistics	R_{wp} = 9.52 %
	GOF = 3.49

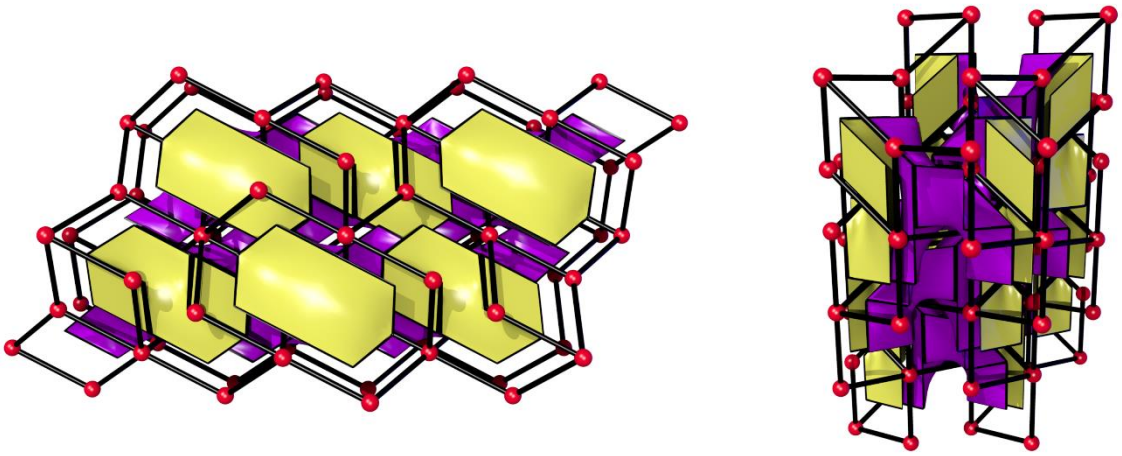

Figure S7. The **esg** net and the tiling found, showing two kinds of tile (yellow and purple), viewed along [010] (left) and [100] (right).

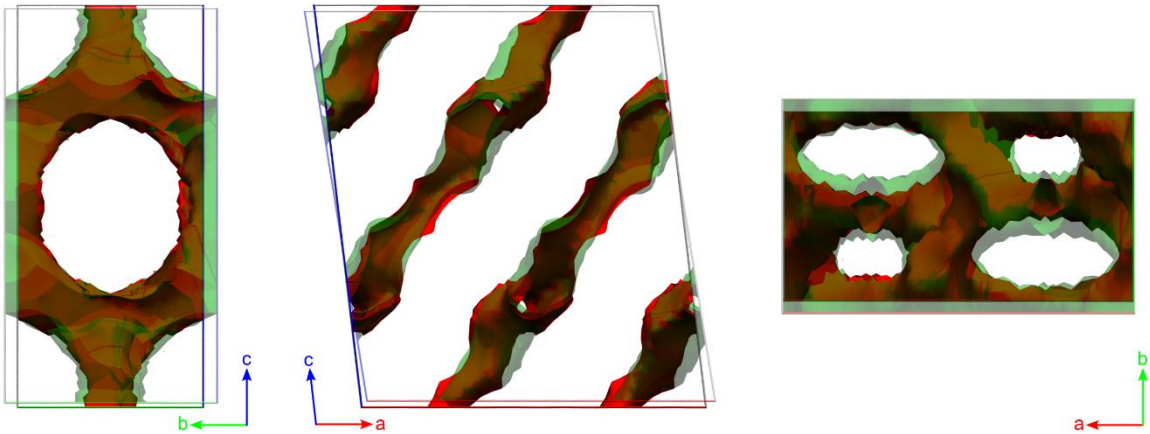

Figure S8. Superimposed figures of the solvent-accessible voids (visualized in MCE2005[1]) for the as-synthesized SU-100 (red) and DEF@SU-100 (green). The views are (from left to right) along [100], [010], and [001]. The solvent accessible void volume increases from 1264 Å^3 (as-synthesized SU-100) to 1596 Å^3 (DEF@SU-100). The expansion occurs in all directions, but is most noticeable when viewing the structure in the *ab*-plane.

Table S5: Crystallographic table for electron diffraction data of SU-100-HT.

Identification Code	SU-100-HT
Wavelength	0.0251 Å
Crystal system	Monoclinic
Space group	*I*2/*a* (No. 15)
Unit cell dimensions	*a* = 19.00 Å
	b = 10.57 Å
	c = 22.07Å
	β = 99.33°
Volume	4373 Å^3
Z	8
Rotation range	110.18° (-43.04 to 67.14°)
Index ranges	-23 ≤ *h* ≤ 23
	-11 ≤ *k* ≤ 11
	-27 ≤ *l* ≤ 27
Reflections collected	3064
Independent reflections	1561
	[R(int) = 0.3739]
Completeness (to 0.8 Å resolution)	90.03 %
R_1 (ED model) [I > 2σ(I)]	0.2949

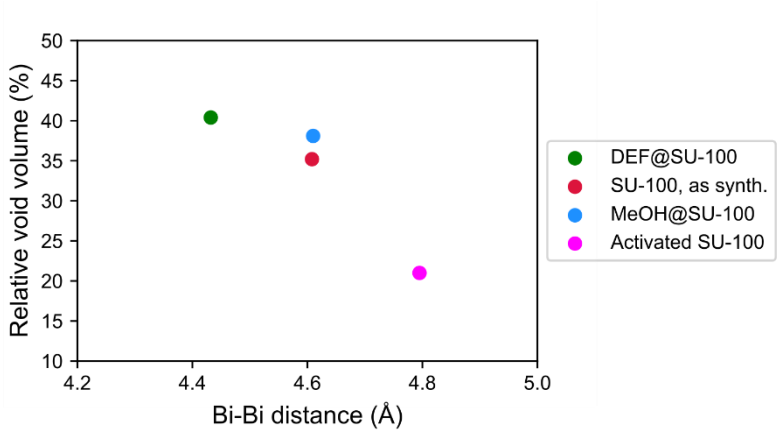

Figure S9. Plot of the calculated void volume (using PLATON's *Calc Solv*) vs. the Bi-Bi distance in the Bi_2O_{12} building unit of SU-100.

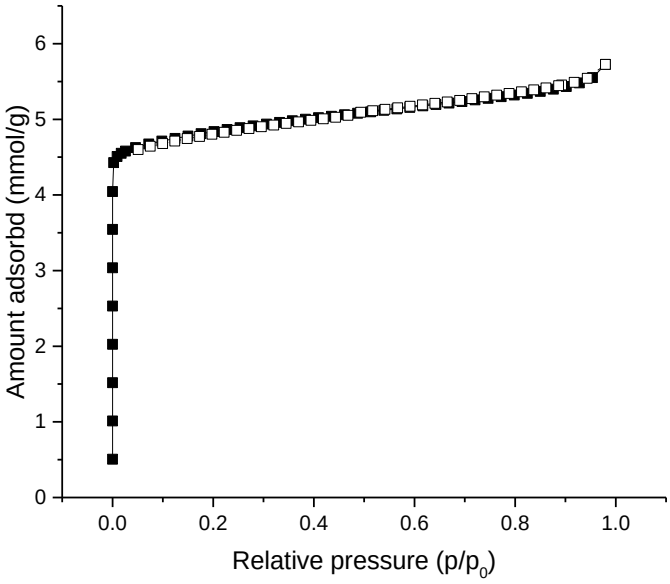

Figure S10. N_2 adsorption/desorption isotherm of SU-100 recorded at liquid N_2 temperature. BET surface area: 385 m^2/g. Langmuir surface area: 483 m^2/g.

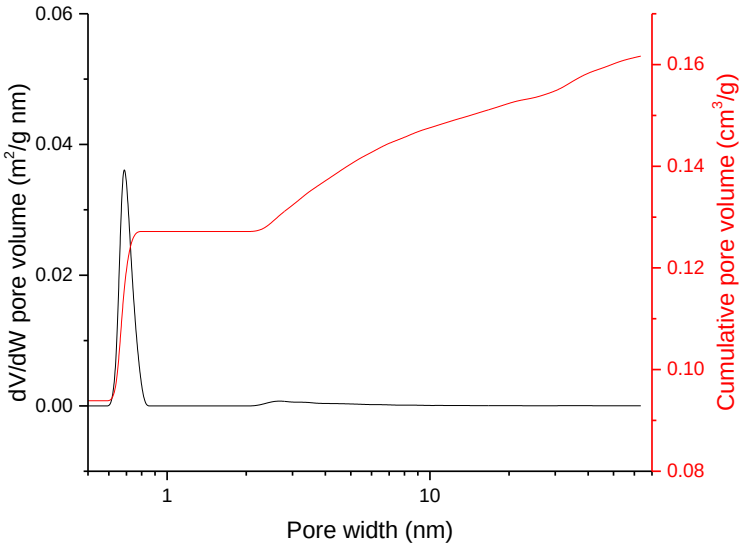

Figure S11. DFT pore size distribution of SU-100.

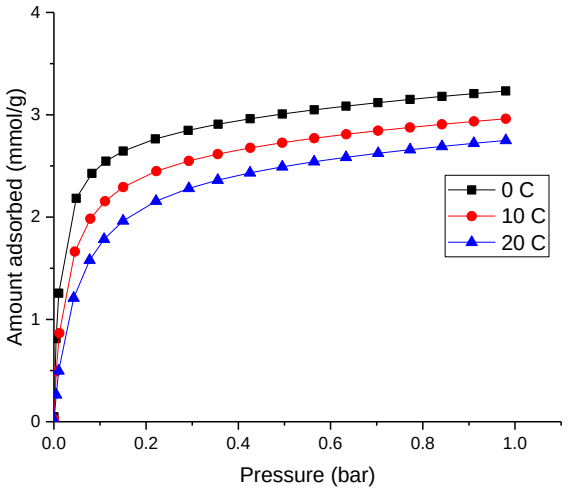

Figure S12. CO_2 adsorption isotherms of SU-100 recorded at 0, 10 and 20 °C

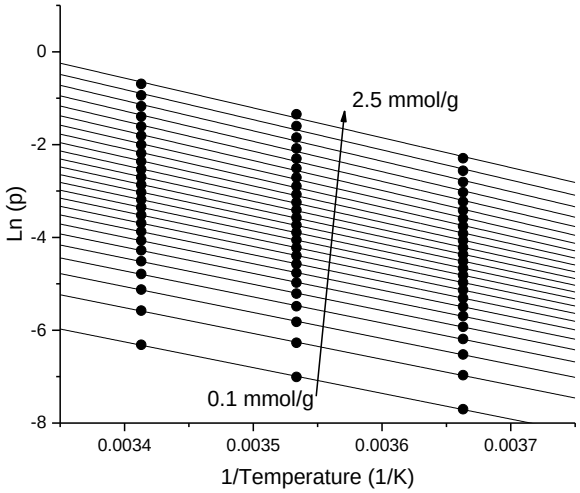

Figure S13. Plot of ln(P) versus 1/T for CO_2 adsorption on SU-100. The heat of adsorption can be calculated from the slope of these lines according to the Clausius-Clapeyron equation.

The heat of CO2 adsorption verses loading on SU-100 was calculated using the Clausius-Clapeyron equation

$$\frac{dln(P)}{d\left(\frac{1}{T}\right)} = -\frac{E_{ads}}{R}$$

where P is the pressure at a particular level of CO_2 loading, T is temperature in K, R is the ideal gas constant and E_{ads} is the heat of CO_2 adsorption. The data used is shown in Figure S13. The CO_2 adsorption isotherms shown in Figure S12 were fitted using the two side Langmuir isotherm model. The fitted Langmuir equation at for each isotherm (at 0, 10 and 20 °C) was used to calculate the equilibrium pressures (P) at CO_2 loading between 0.1 and 2.5 mmol/g at the corresponding temperature. The slope of the ln(P) vs. 1/T plot shown in Figure S13 was fitted with straight lines and the slope of the lines were used to calculate the heat of CO_2 adsorption versus loading. The calculated heat of CO_2 sorption between 0.1 and 2.5 mmol/g loading is shown in Figure S14. The heat of CO_2 adsorption on SU-100 was around 45-55 kJ/mol

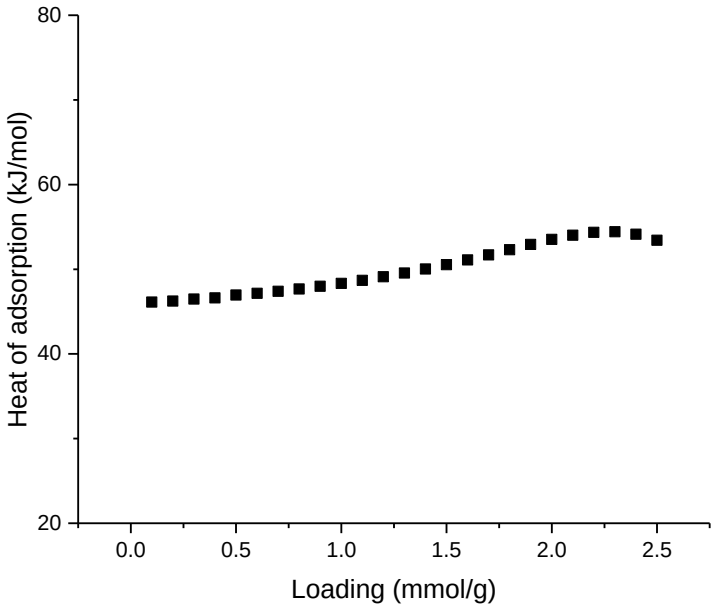

Figure S14. Heat of CO_2 adsorption on SU-100 calculated using the Clausius-Clapeyron equation.

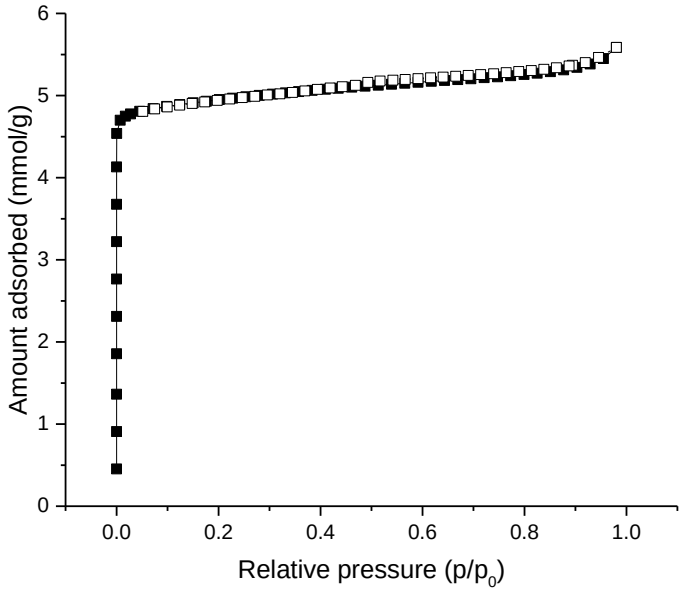

Figure S15. N_2 adsorption/desorption isotherm of SU-100 soaked in water (100 °C, 1 hour) recorded at liquid N_2 temperature. BET surface area: 395 m^2/g. Langmuir surface area: 484 m^2/g.

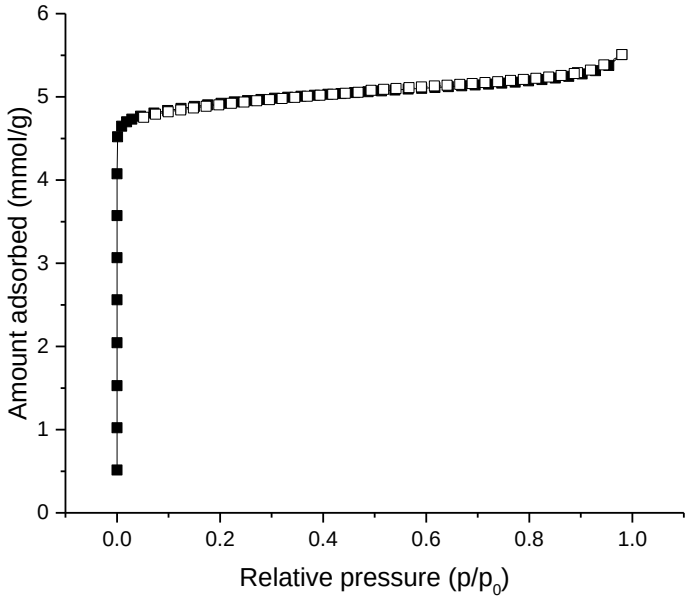

Figure S16. N_2 adsorption/desorption isotherm of SU-100 soaked in toluene (100 °C, 1 hour) recorded at liquid N_2 temperature. BET surface area: 393 m^2/g. Langmuir surface area: 482 m^2/g.

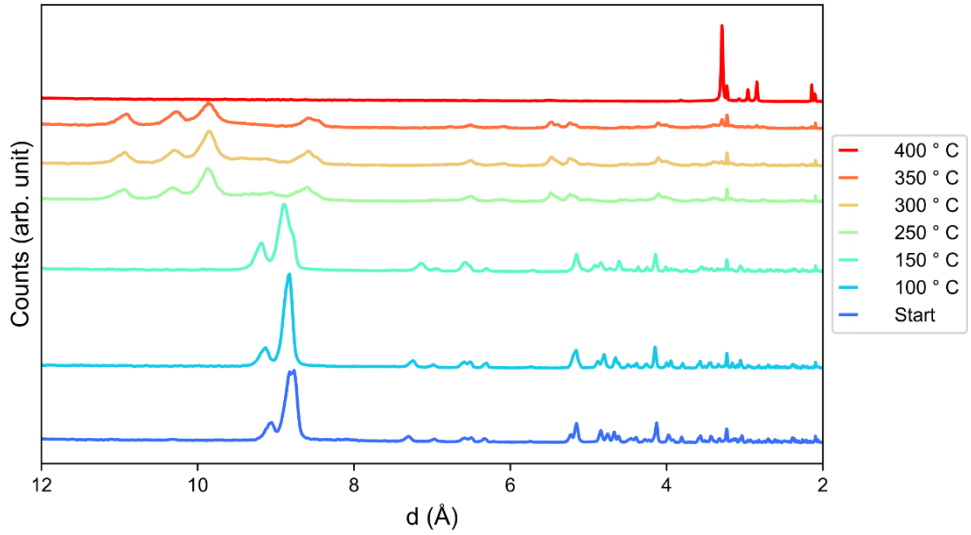

Figure S17. Thermodiffraction measurements of SU-100 in air, showing that large structural changes start to occur above 150 °C. Above 350 °C, the organic material seems to be lost and Bi_2O_3 is acquired.

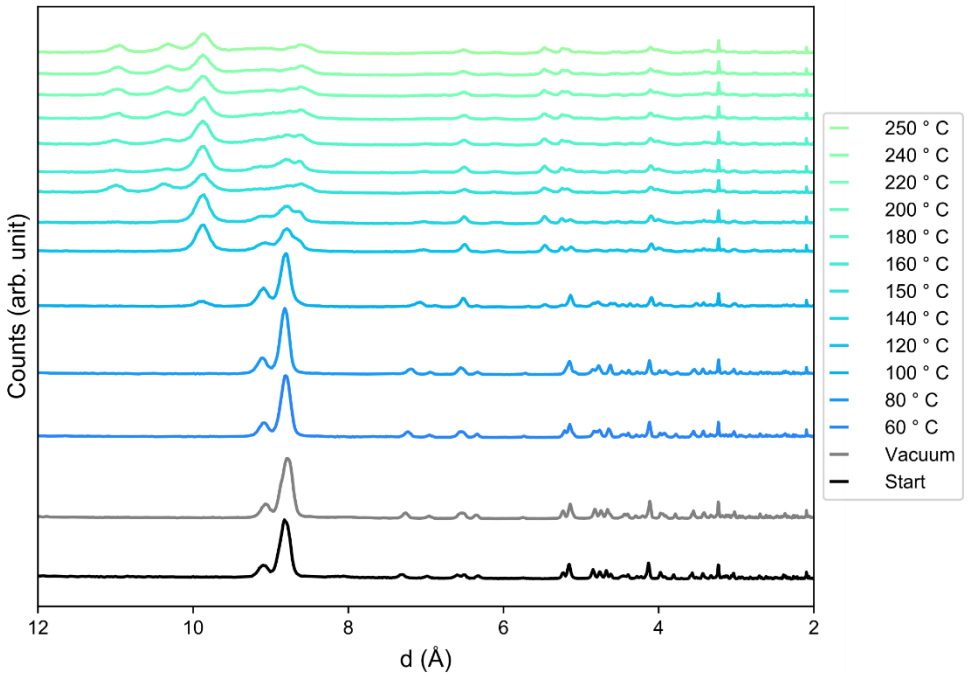

Figure S18. Thermodiffraction measurements of SU-100 under reduced pressure (0.1 bar), showing a virtually unchanged diffraction pattern up to 100 °C. Above 100 °C, large structural changes occur and the strong reflection around 9 Å is gradually lost with increasing temperature. Post-thermodiffraction, the sample was placed in isopropanol, regaining crystallinity (see Figure S19).

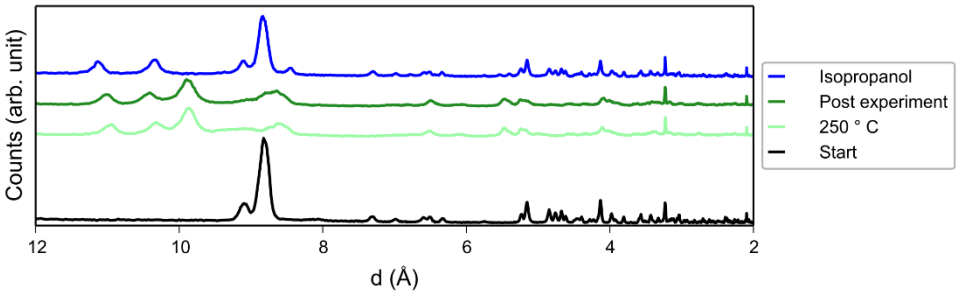

Figure S19. X-ray powder diffraction data on as-synthesized SU-100 (Start), which was then heated to 250 °C, and cooled down to room temperature (Post experiment). A drop of isopropanol was then placed onto the post-thermodiffraction (room temperature and atmospheric pressure) sample of SU-100, showing a diffraction pattern which is somewhat similar to the as-synthesized material. Two additional low-angle peaks are seen. The origin of these two peaks has not been investigated but is suspected to be from an unidentified phase.

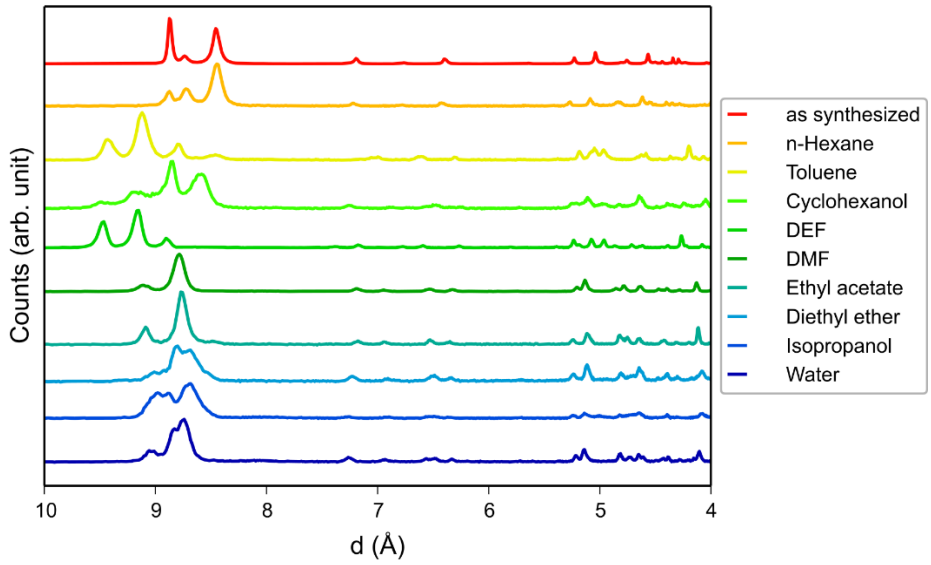

Figure S20. Acquired diffractograms of SU-100 after being immersed in various solvents for 24 hours at room temperature. Branched solvents with more than four non-hydrogen atoms seems to give an apparent increase in the unit cell volume.

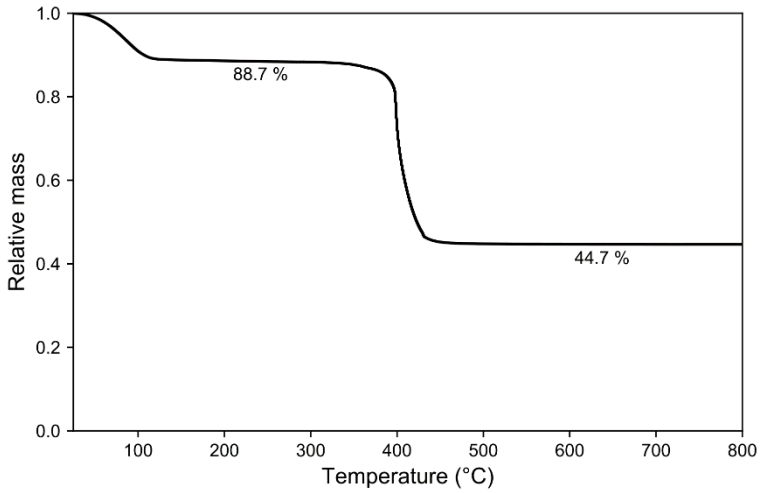

Figure S21. Results from a thermogravimetric analysis of SU-100, showing a weight-loss of 11.3 % from 50-120 °C, matching well with the expected value for two methanol molecules per asymmetric unit (11.5 wt.%). The second weight-loss step of 44.0 % occurs between 350-450 °C (46.6 % expected), where the higher-than-expected remaining mass could be due to unreacted bismuth-species.

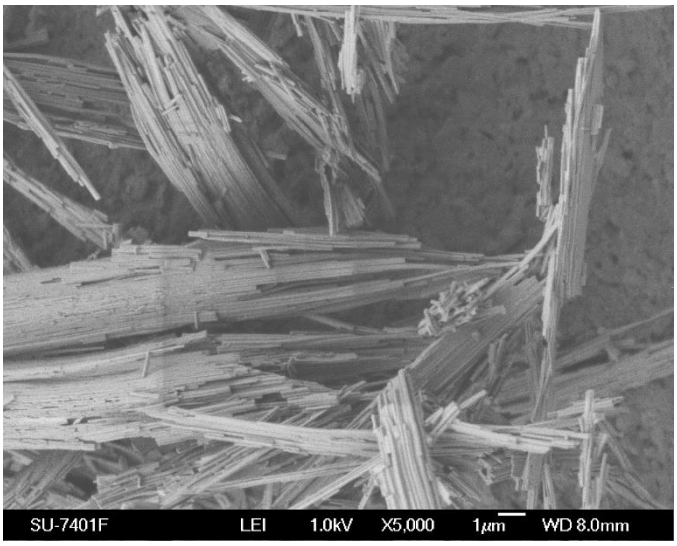

Figure S22. SEM micrograph of Bi_2O_2(HBPT) (**2**), showing aggregates of needle-shaped crystals.

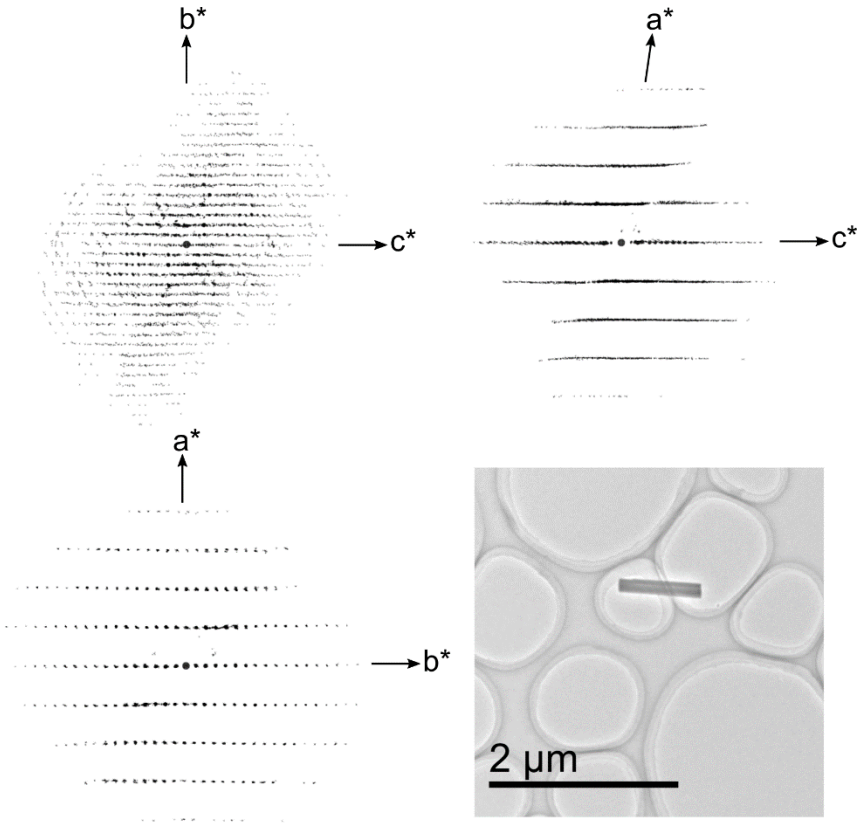

Figure S23. Reciprocal space projections along a*, b* and c*, as well as the crystal used for electron diffraction data collection for Bi_2O_2(HBPT) (**2**).

Table S6: Crystallographic table for electron diffraction data of Bi_2O_2(HBPT) (**2**).

Identification Code	Bi_2O_2(HBPT)
Wavelength	0.0251 Å
Crystal system	Monoclinic
Space group	$P2_1/c$ (No. 14)
Unit cell dimensions	a = 3.99 Å
	b = 15.49 Å
	c = 26.15 Å
	β = 91.66°
Volume	4373 Å^3
Z	4
Rotation range	112.2° (-53.0 to 59.2°)
Index ranges	-4 ≤ h ≤ 4
	-18 ≤ k ≤ 18
	-32 ≤ l ≤ 32
Reflections collected	6944
Independent reflections	2548
	[R(int) = 0.1626]
Completeness (to 0.8 Å resolution)	89.9 %
R_1 (ED model) [I > 2σ(I)]	0.4299

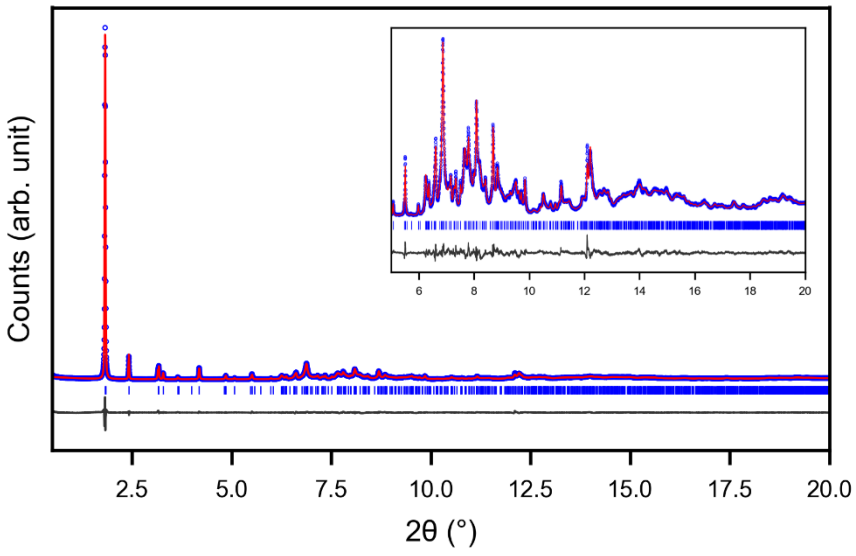

Figure S24. Plot for the structure refinement of Bi_2O_2(HBPT) (**2**). High resolution XRPD data were collected at 11BM at the APS, Argonne National Laboratory, USA, λ = 0.412735 Å.

Table S7. Crystallographic details from X-ray powder diffraction data and structure refinement details for Bi_2O_2(HBPT) (**2**).

Identification code	Bi_2O_2(HBPT) (**2**)
Crystal system	Monoclinic
Space group	$P2_1/c$ (No. 14)
Unit cell dimensions	a = 3.9144(6) Å
	b = 15.015(2) Å
	c = 25.767(4) Å
	β = 91.645(8)°
Volume (Å^3)	1513.8(4) Å^3
Wavelength	0.412735 Å
Refinement method	Profile method
Refinement statistics	R_{wp} = 6.35 %
	GOF = 1.94

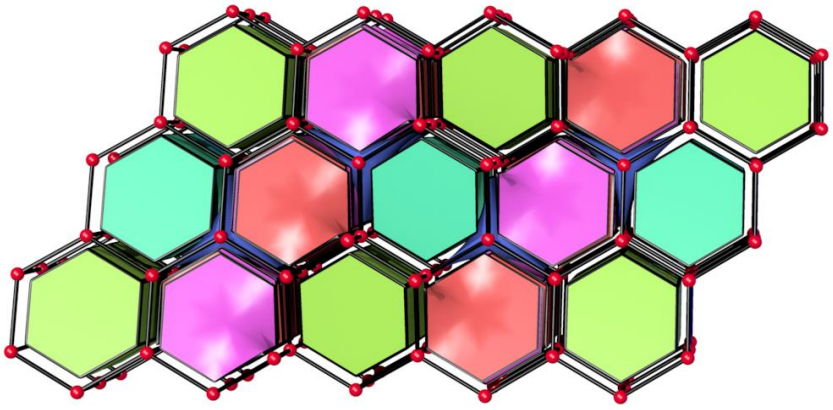

Figure S25. Tiling found for **2** when the organic part is represented as a single 3-c node, viewed slightly off-axis of the [100] direction. The net found has a transitivity of 3685.

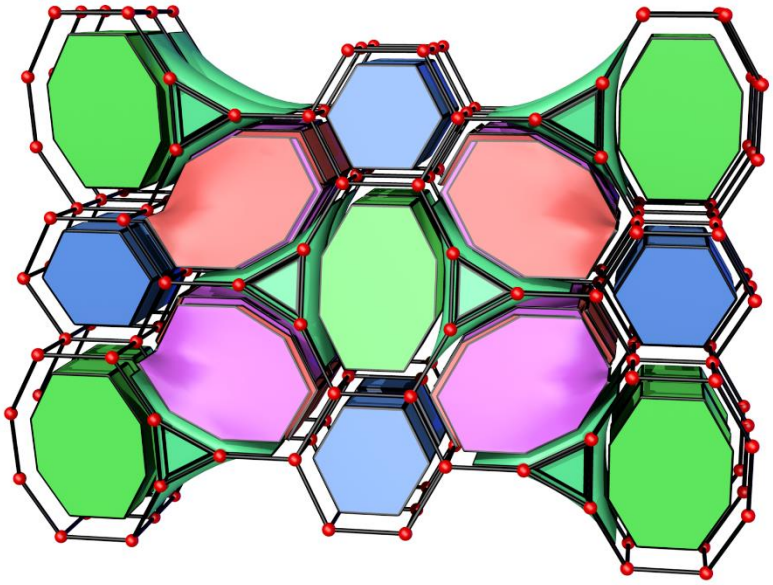

Figure S26. Tiling found for **2** when the organic part is represented as three 3-c nodes, viewed slightly off-axis of the [100] direction. The net found has a transitivity of 6(12)(13)7.

Figure S27. SEM micrograph of $Bi(OH)(H_2BPT)_2(H_2O)_2 \cdot H_2O$ (**3**), showing large bladed crystals together with small amounts of **2**.

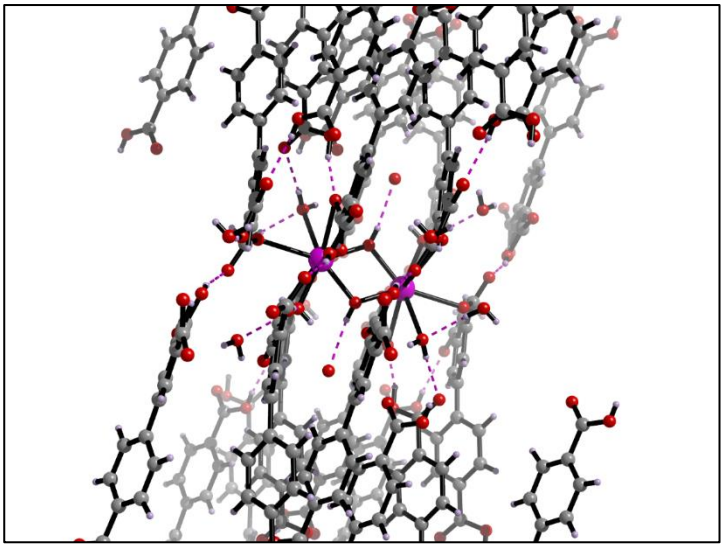

Figure S28. Image showing hydrogen bonds in $Bi(OH)(H_2BPT)_2(H_2O)_2 \cdot H_2O$ (**3**). O···H distances between 1.8 and 2.2 Å are shown in dashed purple lines.

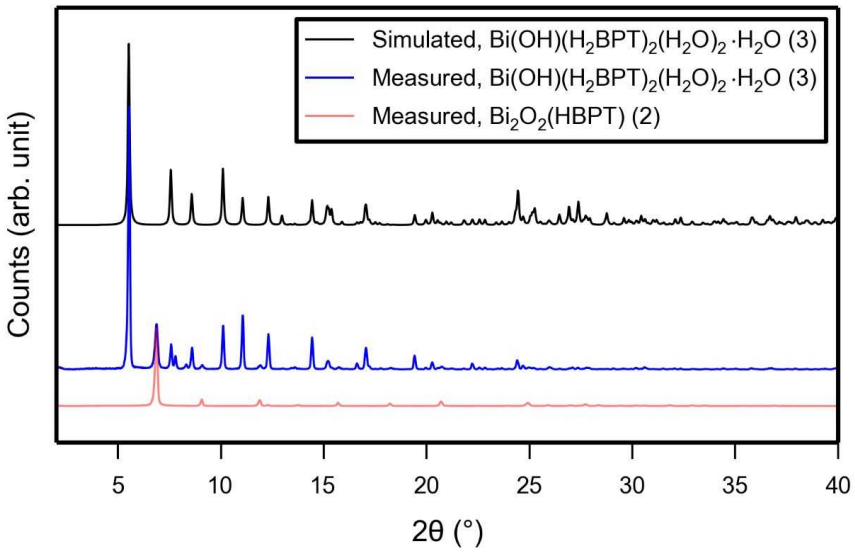

Figure S29. Measured and simulated powder pattern for $Bi(OH)(H_2BPT)_2(H_2O)_2 \cdot H_2O$ (**3**), apprehended as a mixture with **2**, as seen by the measured powder pattern for **3**. There also is a small amount of **4** present (additional reflection around 2θ = 8°).

Table S8. Crystallographic table for single crystal X-ray diffraction data and structure refinement details for $Bi(OH)(H_2BPT)_2(H_2O)_2 \cdot H_2O$ (**3**).

Identification code	$Bi(OH)(H_2BPT)_2(H_2O)_2 \cdot H_2O$ (**3**)
Empirical formula	$C_{30}H_{23}BiO_{16}$
Formula weight	848.46 g mol^{-1}
Temperature	295(2) K
Wavelength	0.71073 Å
Crystal system	Triclinic
Space group	$P\bar{1}$ (No. 2)
Unit cell dimensions	a = 7.3959(3) Å
	b = 11.9364(4) Å
	c = 16.2328(5) Å
	α = 99.343(2)°
	β = 92.285(2)°
	γ = 97.253(2)°
Volume	1400.04(9) $Å^3$
Z	2
Density (calc.)	2.013 g cm^{-3}
Absorption coefficient	6.383 mm^{-1}
F(000)	828
Crystal size	0.20 × 0.02 × 0.02 mm^3
θ range for data collection	2.328 to 27.215°
Index ranges	$-9 \leq h \leq 9$
	$-15 \leq k \leq 15$
	$-20 \leq l \leq 20$
Reflections collected	51476
Independent reflections	6246
	[R(int) = 0.1146]
Absorption correction	Multi-scan
Min. and max. transmission	0.5958 and 0.7460
Data / restr. / param.	6246/2/493
Goodness-of-fit on F^2	1.042
Final R indices [I > 2σ(I)]	R1 = 0.0316,
	wR2 = 0.0580
Largest diff. peak and hole	1.285 and -0.970 e $Å^{-3}$

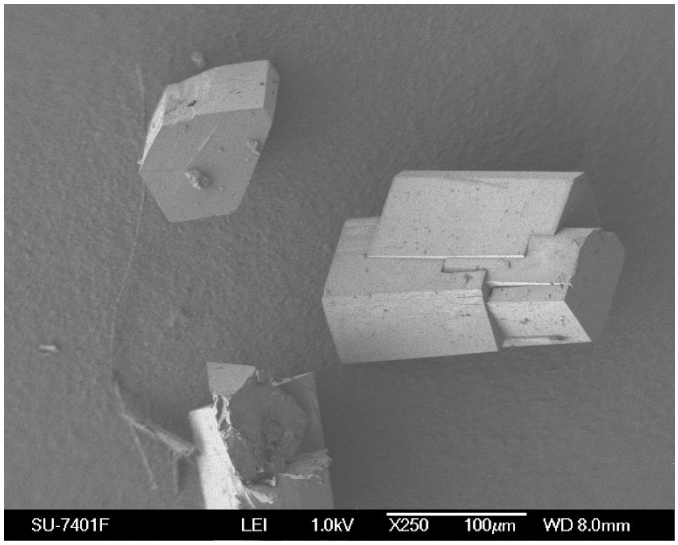

Figure S30. SEM micrograph of $Bi_2(HBPT)_3(H_2O)_3$•H_3BPT (**4**), showing large prismatic crystals.

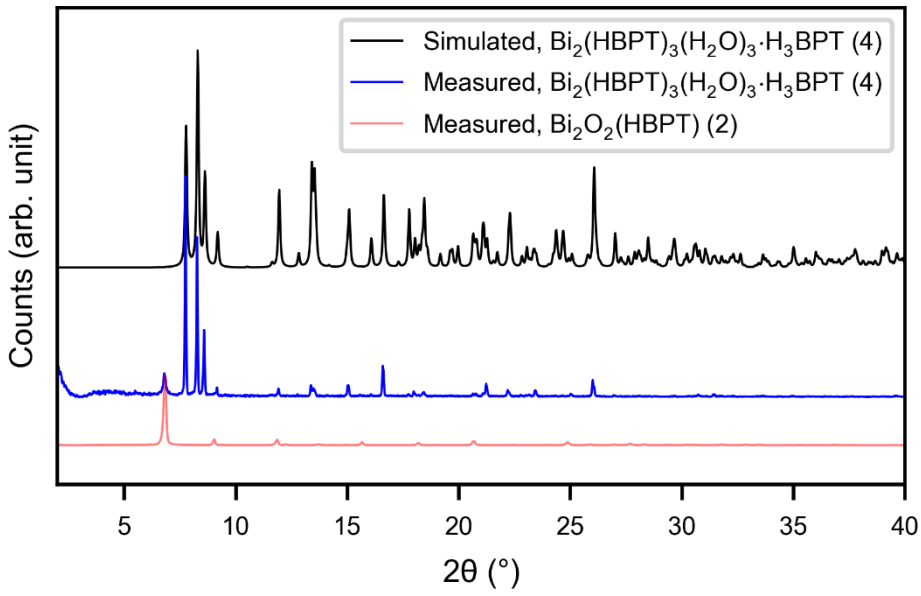

Figure S31. Measured and simulated powder pattern for $Bi_2(HBPT)_3(H_2O)_3$•H_3BPT (**4**), apprehended as a mixture with **2.**

Table S9. Crystallographic table for single crystal X-ray diffraction data and structure refinement for $Bi_2(HBPT)_3(H_2O)_3$•H_3BPT (**4**).

Identification code	$Bi_2(HBPT)_3(H_2O)_3$•H_3BPT (**4**)
Empirical formula	$C_{60}H_{34}Bi_2O_{27}$
Formula weight	1604.83 g mol^{-1}
Temperature	294(2) K
Wavelength	0.71073 Å
Crystal system	Triclinic
Space group	*P*1 (No. 1)
Unit cell dimensions	*a* = 9.9074(4) Å
	b = 11.7713(6) Å
	c = 12.9136(7) Å
	α = 64.992(2)°
	β = 76.477(2)°
	γ = 87.906(2)°
Volume	1323.7(1) $Å^3$
Z	1
Density (calc.)	2.013 g cm^{-3}
Absorption coefficient	6.738 mm^{-1}
F(000)	776
Crystal size	0.20 × 0.10 × 0.10 mm^3
θ range for data collection	2.424 to 27.182°
Index ranges	-12 ≤ *h* ≤ 12
	-15 ≤ *k* ≤ 15
	-16 ≤ *l* ≤ 16
Reflections collected	49759
Independent reflections	11713
	[R(int) = 0.0589]
Absorption correction	Multi-scan
Min. and max. transmission	0.5867 and 0.7455
Data / restr. / param.	11713/180/812
Goodness-of-fit on F^2	1.059
Flack parameter	0.400(7)
Final R indices [I > 2σ(I)]	R1 = 0.0279,
	wR2 = 0.0501
Largest diff. peak and hole	1.607 and -0.725 e $Å^{-3}$

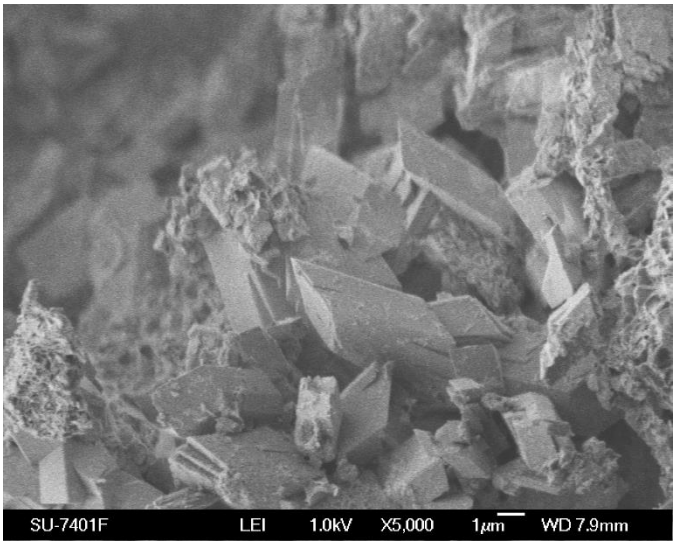

Figure S32. SEM micrograph of $Bi_6O_4(H_2TPTC)_5$ (**5**), showing stubby microscale crystals.

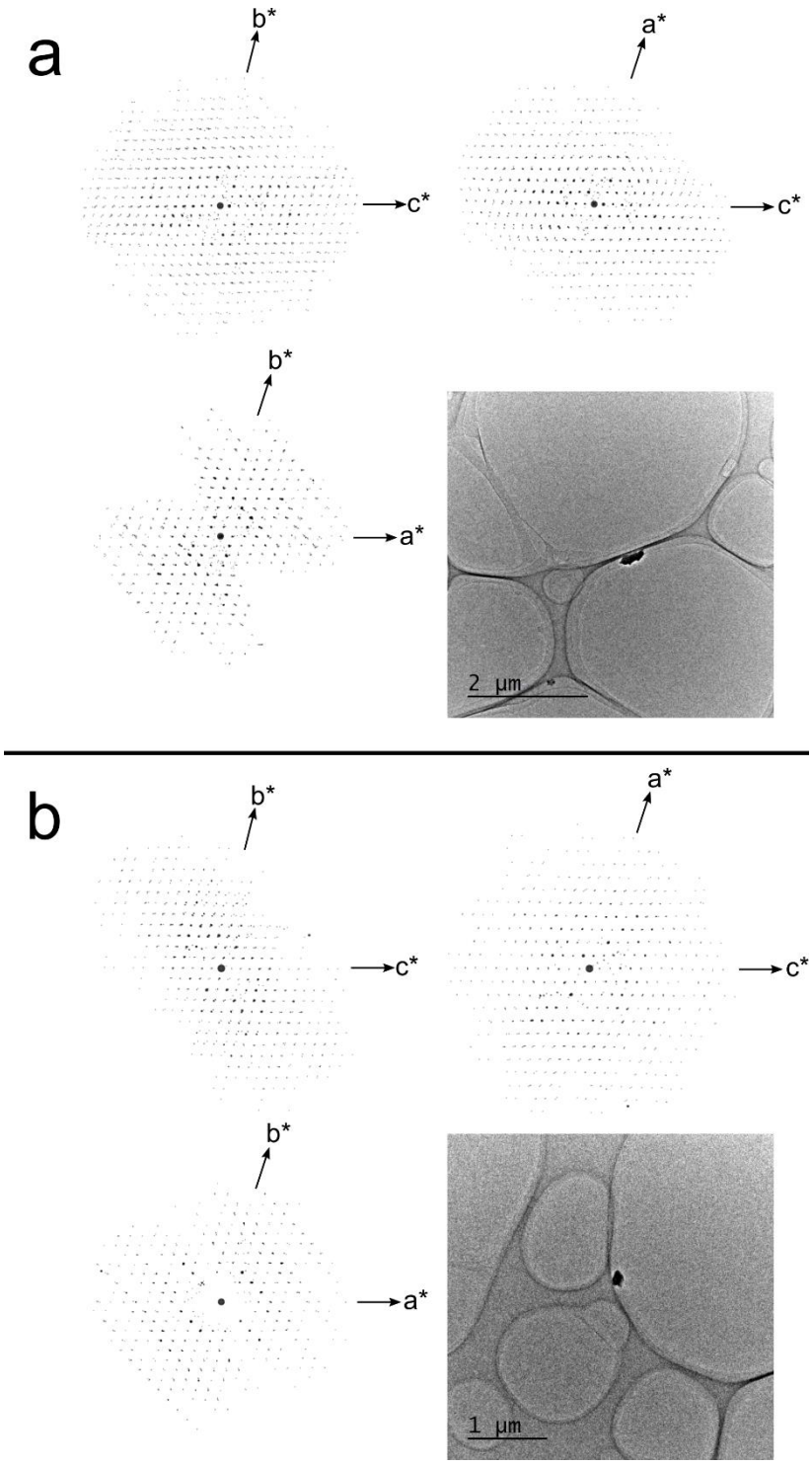

Figure S33. Reciprocal space projection along a*, b* and c*, as well the crystals of $Bi_6O_4(H_2TPTC)_5$ (**5**) used for data collection, for the data sets **a** and **b.**

Table S10: Crystallographic table for merged electron diffraction data of $Bi_6O_4(H_2TPTC)_5$ (**5**).

Identification Code	$Bi_6O_4(H_2TPTC)_5$ (**5**)
Wavelength	0.0251 Å
Crystal system	Triclinic
Space group	$P\bar{1}$ (No. 2)
Unit cell dimensions	a = 11.90 Å
	b = 14.49 Å
	c = 16.10 Å
	α = 102.50°
	β = 106.82°
	γ = 105.62°
Volume	2425 Å^3
Z	2
Index ranges	$-11 \leq h \leq 11$
	$-14 \leq k \leq 14$
	$-16 \leq l \leq 16$
Reflections collected	10729
Independent reflections	3883
	[R(int) = 0.2126]
Completeness (to 1.0 Å resolution)	71.9 %
R_1 (ED model) [I > 2σ(I)]	0.1826

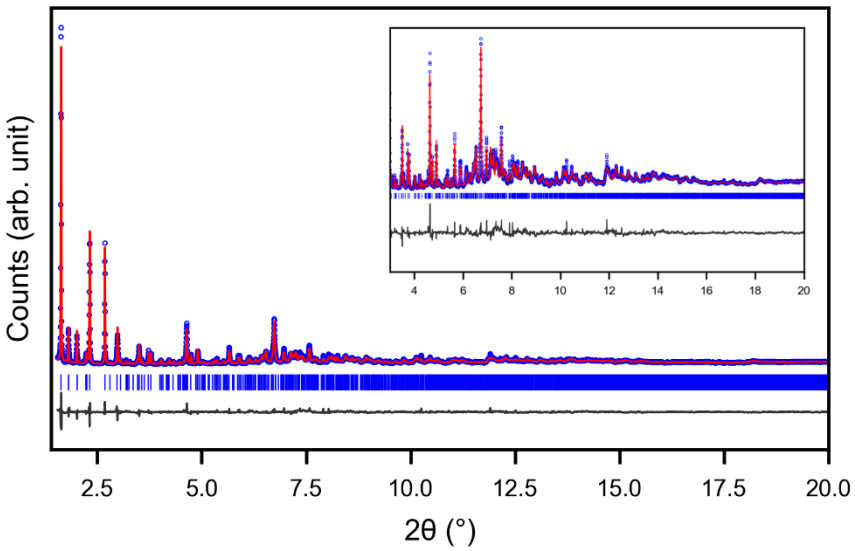

Figure S34. Plot for the structure refinement of $Bi_6O_4(H_2TPTC)_5$ (**5**). High resolution XRPD data were collected at 11BM at the APS, Argonne National Laboratory, λ = 0.412735 Å.

Table S11. Crystallographic details from X-ray powder diffraction data and structure refinement details for $Bi_6O_4(H_2TPTC)_5$ (**5**).

Identification code	$Bi_6O_4(H_2TPTC)_5$ (**5**)
Crystal system	Triclinic
Space group	$P\bar{1}$ (No. 2)
Unit cell dimensions	a = 11.874(3) Å
	b = 14.349(4) Å
	c = 16.022(4) Å
	α = 102.318(7)°
	β = 106.892(7)°
	γ = 106.178(5)°
Volume (Å^3)	2376(1) Å^3
Wavelength	0.412735 Å
Refinement method	Profile method
Refinement statistics	R_{wp} = 10.00 %
	GOF = 3.02

Table S12. Summary of crystallographic details and CCDC numbers of all presented structures in this work.

Formula	**Bi_2O_2(HBPT)**	**Bi(OH)(H_2BPT)$_2$ (H_2O)$_2$•H_2O**	**Bi_2(HBPT)$_3$(H_2O)$_3$ •H_3BPT**	**Bi_6O_4(H_2TPTC)$_5$**	**Bi(BPT) •2MeOH**	**Bi(BPT) •3MeOH**	**Bi(BPT) •DEF**
CCDC number	1926729	1926730	1926731	1926732	1926733	1926734	1926735
Sample name					SU-100 as-synthesized	MeOH@SU-100	DEF@SU-100
Sample number	**2**	**3**	**4**	**5**	**1**	MeOH@**1**	DEF@**1**
Space group	*P*2$_1$/*c*	*P*-1	*P*1	*P*-1	*I*2/*a*	*I*2/*a*	*I*2/*a*
***a* / Å**	3.9144(6)	7.3959(3)	9.9074(4)	11.874(3)	17.854(3)	18.0213(6)	18.018(1)
***b* / Å**	15.015(2)	11.9364(4)	11.7713(6)	14.349(4)	9.613(2)	10.0372(4)	10.8566(8)
***c* / Å**	25.767(4)	16.2328(5)	12.9136(7)	16.022(4)	21.047(4)	21.2624(8)	20.478(1)
***alpha* / °**	90	99.343(2)	64.992(2)	102.318(7)	90	90	90
***beta* / °**	91.645(8)	92.285(2)	76.477(2)	106.892(7)	96.771(2)	99.206(1)	99.1116(5)
***gamma* / °**	90	97.253(2)	87.906(2)	106.178(5)	90	90	90

(1) Rohlíček, J.; Hušák, M. MCE2005 - A New Version of a Program for Fast Interactive Visualization of Electron and Similar Density Maps Optimized for Small Molecules. *J. Appl. Crystallogr.* **2007**, *40* (3), 600–601.